

# Generation of Road Reference Heading using GPS Trajectories for Accurate Lane Departure Detection

Shahnewaz Chowdhury, Md. Touhid Hossain and M. I. Hayee

*Department of Electrical Engineering, University of Minnesota Duluth, Duluth, MN 55812, U.S.A.*

**Keywords:** Lane Departure Warning System, Road Reference Heading, GPS Trajectory.

**Abstract:** Lane departure warning system (LDWS) has significant potential to reduce crashes on roads. Most existing commercial LDWSs use image processing techniques with or without Global Positioning System (GPS) technology and/or high-resolution digital maps to detect unintentional lane departures. However, the performance of such systems is compromised in unfavourable weather or road conditions e.g., fog, snow, or irregular road markings. Previously, the authors proposed and developed an LDWS using a standard GPS receiver without any high-resolution digital maps. The previously developed LDWS relies on a road reference heading (RRH) of a given road extracted from an open-source low-resolution mapping database to detect an unintentional lane departure. This method can detect true lane departures accurately but occasionally gives false alarms i.e., it issues lane departure warnings even if a vehicle is within its lane. The false alarms occur due to the inaccuracy of RRH originated from inherent lateral error in open-source low-resolution maps. To overcome this problem, now authors propose a novel algorithm to generate an accurate RRH for a given road using a vehicle's past trajectories on that road. The newly proposed algorithm to generate an accurate RRH for any given road has been integrated with the previously developed LDWS and extensively evaluated in the field to detect unintentional lane departures. The field test results show that the newly developed RRH generation algorithm significantly improves the performance of the previously developed LDWS by accurately detecting all true lane departures while practically reducing the frequency of false alarms to zero.

## 1 INTRODUCTION

Lane departure warning system (LDWS) has significant potential to reduce accidents. According to the American Association of State Highway and Transportation Officials (AASHTO), almost 60% of fatal accidents are caused by an unintentional lane drifting of a vehicle on major roads (AASHTO: Driving down lane-departure crashes: A national priority, 2008). A recent study which compared crashes with and without an LDWS found that an in-vehicle LDWS was helpful in reducing crashes of all severities by 18%, with injuries by 24%, and with fatalities by 86% (J Cichino, 2018). Systems which predict the driver's attentive state and intent of lane change (D. D. Salvucci, 2004, N. Kuge et al. 1998, J. McCall et al. 2004) and provide map-based route guidance and/or warning about unintentional lane departure (F. Heimes et al. 2002, W. Kwon et al. 2002), are also useful to reduce major road crashes.

Most available LDWSs rely on image processing technology using a camera or an optical scanning

device to estimate a vehicle's lateral shift within a lane to detect an unintentional lane departure (Xiangjing An et al. 2006, Pei-Yung Hsiao et al. 2006, B. Yu et al. 2008, Y. C. Leng et al. 2010, P. Lindner et al. 2009). Although advanced image processing techniques work well in diminished lighting scenarios (McCall et al. 2006, Daimler, 2018) the performance of image processing based LDWSs deteriorates in unfavourable weather and road conditions e.g., fog and snow-covered or worn-out road marking signs. To overcome these problems and improve performance, Global Positioning System (GPS) technology is integrated within vision based LDWS. However, such systems use differential GPS technology and/or inertial navigation sensors as well as high-resolution digital maps to estimate a vehicle's lateral shift in its lane making such systems more complex and expensive to implement (Clanton, 2009).

Previously, the authors proposed a novel method to accurately detect an unintentional lane departure using a standard GPS receiver and commonly available open-source low-resolution digital maps

(Faizan et al. 2019). The previously proposed method estimates vehicle’s lateral shift by comparing vehicle’s heading acquired by standard GPS receiver to a road reference heading (RRH) extracted from an open-source digital map. Although this system works well to successfully detect unintentional lane departure, occasionally, it generates false alarms i.e., it wrongfully issues lane departure warnings even if the vehicle is within its lane (Faizan et al. 2019). The false alarms occur due to inherent error in open-source digital maps which resulted in an error in the corresponding RRH of the given road extracted from such maps. The authors now propose another method to generate an accurate RRH for any given road using a vehicle’s past GPS trajectories on that road without relying on open-source digital maps.

Previously, many techniques have been proposed to process GPS trajectories to generate a routable road network or create a complete digital road map using graph and structured learning theory and/or statistical analysis (Cao et al. 2009, Guo et al. 2007, Chen et al. 2008, Guo et al. 2010, Shi et al. 2009, Huang et al. 2018). In this paper, a novel algorithm is proposed to generate an accurate RRH from a vehicle’s past GPS trajectories to improve the performance of the previously proposed lane departure detection method (16). The test results show that the newly proposed algorithm significantly improves the performance of the previously proposed lane departure detection method by accurately detecting all true lane departures while practically reducing the frequency of false alarms to zero.

The rest of the paper is organized as follows. Section 2 describes the system architecture of the proposed lane departure system using RRH generated from a vehicle’s past trajectories. The details of the newly proposed RRH generation algorithm are provided in Section 3, and the field test results are discussed in Section 4. The conclusions are given in Section 5.

## 2 SYSTEM ARCHITECTURE

The newly proposed algorithm generates RRH for any given road using a vehicle’s one or more past trajectories on that road acquired by a standard GPS receiver. Once an RRH for a given road is generated, it can be used to detect any future unintentional lane departure of a vehicle as illustrated in Figure 1a, where the dashed line represents a vehicle’s past trajectory which can be used to generate RRH for the road to detect an unintentional lane departure e.g., as represented by a dotted line in Figure 1a.

The architecture of the proposed system combining the previously developed lane departure detection method and the newly proposed RRH generation algorithm is shown in Figure 1b where the GPS receiver acquires longitude and latitude of a moving vehicle’s position in real-time to be used by both processors. The Processor 1 uses a sufficient length of a GPS trajectory on a given road to generate an RRH for that road using the newly developed algorithm.

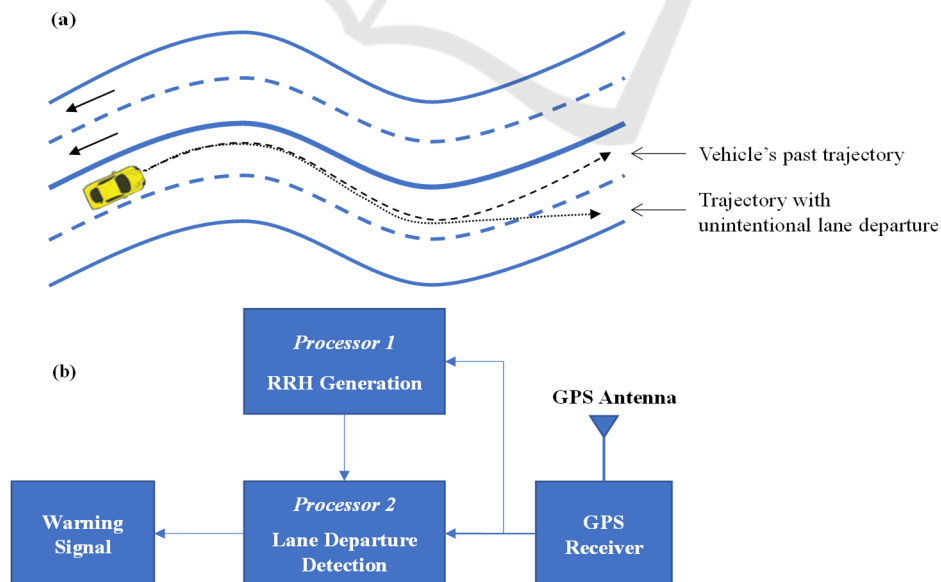


Figure 1: (a) Conceptual diagram showing how a past trajectory (black dashed line) of a given vehicle can serve to generate RRH to detect its unintentional lane departure in future (black dotted line), and (b) the system architecture of LDWS using the newly proposed algorithm to generate RRH from a vehicle’s past GPS trajectories.

On the other hand, Processor 2 works in real-time to detect unintentional lane departure using the previously proposed lane departure detection method except that it uses the RRH generated by Processor 1 using one or more past GPS trajectories as opposed to the RRH extracted from an open-source low-resolution map as was used in . The Processor 2 can detect an unintentional lane departure of any vehicle on a given road if the vehicle has been driven on that road at least once before so that the necessary RRH for that road has already been generated by Processor 1. Please note that the proposed algorithm is suitable to be integrated into smartphone Apps e.g., Waze, Google Maps, or Apple Maps to take advantage of the vast database of multiple GPS trajectories of a broader road network. This can enable any vehicle to detect an unintentional lane departure on any road even if the vehicle is driven on that road for the first time.

### 3 RRH GENERATION ALGORITHM

Any typical road segment may consist of a combination of straight and curve road sections. Usually, a road is not curved abruptly, therefore, a transition section exists between a straight and a curve section. The proposed algorithm to generate a vehicle's trajectory into a useful RRH works in three stages. In the first stage, all straight, curve, and transition sections of any road are identified from the given GPS trajectory on that road. In the second stage, each identified section is characterized with a set of optimized parameters defining road reference heading value at each point on that road section. In the third stage, all individual road sections are combined to obtain a composite RRH for that road.

#### 3.1 Identification of Various Sections

The heading for a straight road section remains constant while it changes uniformly for a curve section. Similarly, the differential heading for a straight section is zero while it has a non-zero constant value for a curve section with larger values for sharper curves. A typical vehicle trajectory acquired by a standard GPS receiver consists of its position coordinates at fixed time intervals (typically every 100 msec). Any two consecutive position coordinates of a moving vehicle on a given road can be used to obtain heading and differential heading of the road at that point.

The proposed algorithm uses differential heading to identify various sections present in a given road by first identifying all straight sections where differential heading remains zero followed by curve sections where differential heading is a non-zero constant. The transition sections are identified at the end.

To illustrate the section identification process, heading and differential heading calculated from a typical GPS trajectory versus distance are shown in Figure 2a and 2b, respectively. The GPS trajectory was acquired using a standard GPS receiver with a UBlox LEA-6 chipset on a 4.2 km section of Interstate I-35 while driving at 70 MPH. The heading at each point of the given road, calculated from a vehicle's GPS trajectory, exhibits a high-frequency noise over distance caused by inherent GPS error which is further accentuated in differential heading values as shown in Figure 2b. This high-frequency noise can be reduced by moving average method using more than two consecutive GPS points for heading and differential heading calculation. For the proposed algorithm, a 9-point moving average was used to reduce the standard deviation of differential heading to  $0.03^\circ$ .

##### 3.1.1 Identification of Straight Sections

Although the average differential heading of a straight section is zero, the instantaneous differential heading at any point of a straight section fluctuates around zero due to GPS noise. This fluctuation remains within the boundaries of  $\pm 0.09^\circ$  or three times the standard deviation of differential heading as shown in Figure 2b. The proposed algorithm identifies straight sections by comparing the differential heading with a threshold of  $\pm 0.09^\circ$  as shown by dashed red line in Figure 2b. Whenever the differential heading exceeds the threshold of  $\pm 0.09^\circ$  in either direction, the crossing points are marked as the beginning and ending points of the straight sections of the road. All such points are shown by vertical blue dashed lines in Figure 2, identifying a total of four straight sections from the given trajectory which are marked as S1, S2, S3, and S4.

There is no lane change present in the trajectory of Figure 2. However, in reality, a vehicle may change lanes while traveling on a multiple lane road. The lane changes present in any given trajectory may wrongfully be considered as road curvature on that road. However, the differential heading during any typical lane change does not exceed the threshold of  $\pm 0.09^\circ$ . Therefore, the proposed algorithm can correctly identify all straight sections of the road even if lane changes are present in each trajectory.

### 3.1.2 Identification of Curve Sections

There is usually a curve and two transition sections present between any two consecutive straight sections. To identify a curve section between any two consecutive straight sections, the proposed algorithm calculates a path average differential heading (PADH) between the ending point of the first and beginning point of the second of the two consecutive straight sections.

The value of calculated PADH will be slightly smaller than the true PADH value of the curve section alone because this is calculated for the curve section including the two adjoining transition sections on each side of the curve as illustrated in Figure 3, where a zoomed-in portion of the trajectory of Figure 2 is reproduced showing only the first curve section surrounded by two straight sections (S1 and S2) and corresponding transition sections. To identify the beginning and ending points of a curve section alone, a set of two points between two consecutive straight sections (one on each side) are identified where the differential heading value is closest to the calculated PADH.

The beginning and ending points of a curve section identified this way will still not be the true beginning and ending points of the curve because the PADH value used to identify these points was calculated for the curve section including the two

transition sections. Therefore, a second iteration of the same routine is performed by calculating a new PADH value between the two points identified in the first iteration. The new PADH value calculated in the second iteration is more likely to be closer to the true PADH value of the curve section alone because it is calculated for the curve section including only the extreme ends of the transition sections on both sides. This process can be repeated, however, beyond two iterations, the beginning and ending points of a curve section do not change significantly. Using this method, all curve sections can be identified in any given GPS trajectory. A total of three curve sections (C1, C2, and C3) were identified in the given GPS trajectory of Figure 2. Please note that the proposed algorithm can correctly identify all curve sections in a given trajectory even when a lane change is present for the same reason as explained for straight section.

### 3.1.3 Identification of Transition Sections

After identifying the beginning and ending points of all straight and curve sections, all remaining portions of the trajectory are marked as transition sections. The beginning and ending points of any transition section will be the ending and beginning points of adjoining straight and curve sections as shown for the transition sections T1 and T2 in Figure 3. Similarly, all transition sections in any given trajectory are identified.

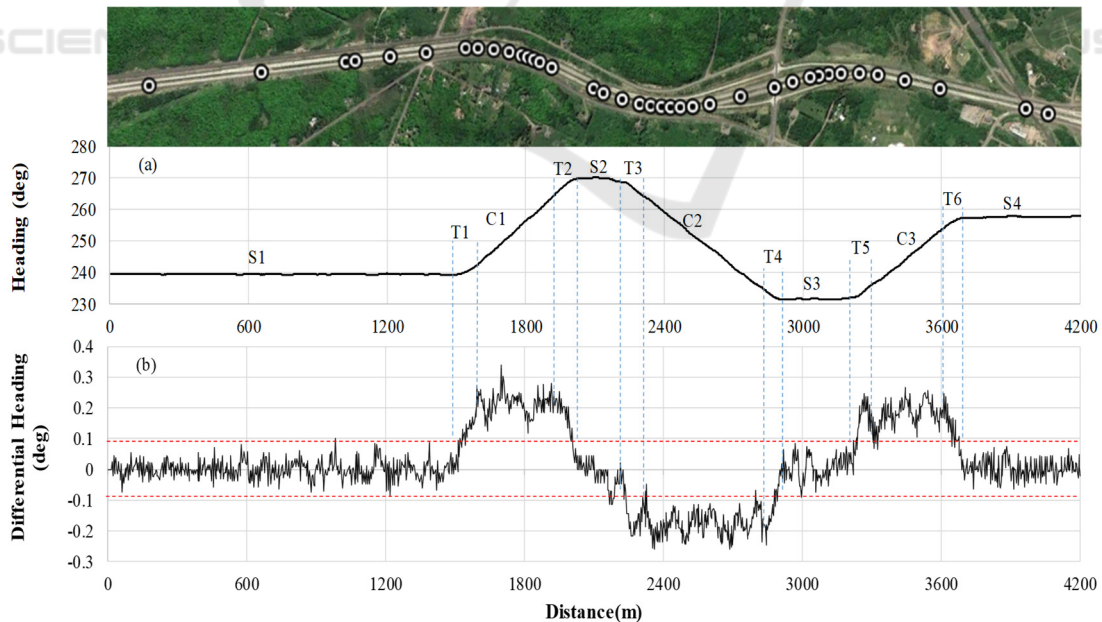


Figure 2: (a) Vehicle heading and (b) differential heading vs. distance for a vehicle's trajectory acquired by a standard GPS receiver on a 4.2 km segment of Interstate I-35. The picture of Google Map of the relevant portion of the road is shown on the top.

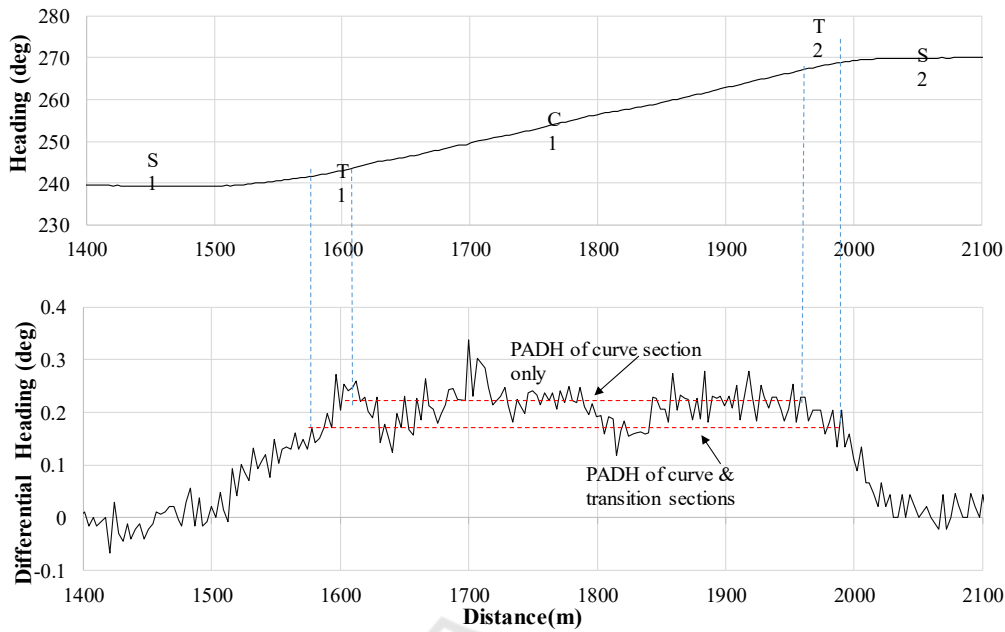


Figure 3: (a) Vehicle heading and (b) differential heading vs. distance for a small portion of the trajectory of Figure 2. This portion includes a part of first straight section, S1, T1, C1, T2, and a part of S2.

### 3.2 Characterization of Various Sections

After identifying all individual sections of the road from a given trajectory, each section is characterized separately with a proper set of parameters to define RRH at each point of the given road section. Each straight section is characterized with a path average heading (PAH) as heading remains the same for the entire length of a straight section. Similarly, heading of a curve section changes uniformly with distance, therefore, it is characterized with a path average heading slope (PAHS) and an initial heading (IH) i.e., the heading at the beginning point of the curve section to completely define RRH at each point of the curve section. For a transition section, heading neither remains the same as in a straight section nor does it change uniformly with distance as in a curve section suggesting that a transition section should be characterized as a second-order polynomial. However, the length of a typical transition section is usually too small to characterize it as a second-order polynomial. Furthermore, the incremental accuracy of RRH with a second-order characterization is negligibly small. Therefore, the proposed algorithm characterizes each transition section just like a curve section i.e., with IH and PAHS values. Please note that the PAHS value of a transition section is different from the PAHS value of the adjoining curve section.

#### 3.2.1 Characterization of Straight Sections

Each straight section is initially characterized with a PAH value, between the beginning and ending points of a straight section, calculated using equation 1, where  $h_n$  is the vehicle heading between any given point  $n$  and its previous point, and  $d_n$  is the distance between the two points.

$$PAH = \frac{\sum d_n h_n}{\sum d_n} \quad (1)$$

However, the initially assigned value of PAH for any given straight section may not be the optimal value. To find the optimal value of PAH for a straight section, the heading error between the vehicle heading and PAH should be minimized. The value of PAH is varied in small increments around its initially assigned value and root mean square of heading error (RMSHE) is calculated for each value of PAH using equation 2, where  $h_{ref}$  is the RRH i.e., PAH for a straight section.

$$RMSHE = \sqrt{\langle |h_n - h_{ref}|^2 \rangle} \quad (2)$$

The RMSHE for the first straight section (S1) of Figure 2 is shown in Figure 4a for varying values of PAH. The RMSHE remains almost flat for a wide range of PAH values suggesting that optimal value of PAH is not very sensitive to small changes. Although minimizing RMSHE would result in an optimized

value of  $h_{ref}$  for a given straight section, the objective at hand is to minimize ALS for each section because ALS is to be used to detect unintentional lane departure (Faizan et al. 2019). Therefore, the absolute value of ALS ( $|ALS|$ ) is also calculated by varying PAH value for each straight section using equation 3.

$$|ALS| = \left| \sum d_n \sin(h_n - h_{ref}) \right| \quad (3)$$

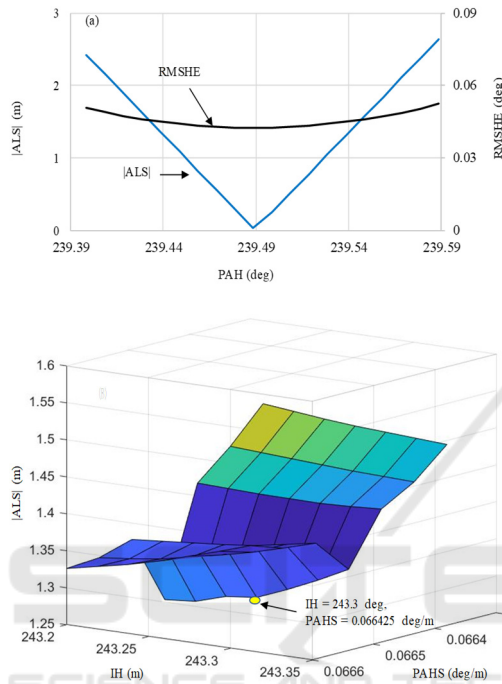


Figure 4: (a) RMSHE and  $|ALS|$  vs. PAH for the straight section S1 showing optimal value of PAH, and (b) a surface plot of  $|ALS|$  vs. IH and PAHS for the curve section C1 showing optimal combination of IH and PAHS values.

The calculated value of  $|ALS|$  for different PAH values around its initially assigned value for the section S1 is also shown in Figure 4a, along with RMSHE values, revealing a clear minimum. The optimal value of PAH (239.50°) not only minimizes  $|ALS|$  but also falls within the flat minimum range of RMSHE. The same general trend was true for all straight sections of the trajectory. Using this method, any straight section can be characterized with an optimal value of PAH.

Please note that the heading can change significantly as opposed to differential heading during a lane change present in a trajectory. Therefore, the optimal value of PAH can be adversely affected for a straight section if a lane change is present. The proposed algorithm can detect the location and span length of such a lane change and optimize the PAH value excluding the lane change portion of the section.

### 3.2.2 Characterization of Curve Sections

As described earlier, each curve section is characterized with two parameters, i.e., IH and PAHS. An initial value of IH is assigned as the heading at the beginning point of any curve section and the initial value of PAHS is assigned using equation 4, where  $h_n$  is the heading between any given point  $n$  and its previous point, and  $h_{n-1}$  is the heading between point  $n-1$  and its previous point.

$$PAHS = \frac{\sum d_n \times \frac{h_n - h_{n-1}}{d_n}}{\sum d_n} \quad (4)$$

After initial values are assigned to both IH and PAHS for a curve section, they are optimized by minimizing  $|ALS|$  by varying both IH and PAHS values in small increments around their initially assigned values. The optimization process is illustrated in Figure 4b, where  $|ALS|$  is plotted versus IH and PAHS as a surface plot for the curve section C1. Please note that the resulting optimal values of IH and PAHS are 243.30° and 0.066425 deg/m, respectively, and are noticeably different from their corresponding initially assigned values (243.26° and 0.066475 deg/m). Using the same method, all other curve sections are optimized. Please note that the optimization of a curve section in the presence of a lane change is performed the same way as described for straight section.

### 3.2.3 Characterization of Transition Sections

As discussed earlier, each transition section is characterized as it is a curve section. Therefore, it should be initially assigned with two parameters, i.e., IH and PAHS, and their optimization process should be like that of a curve section. However, if both parameters are optimized independently then there is a possibility of an abrupt change of heading at corner points where transition section adjoins a straight or a curve section. This is because the end points of any transition section are the same as the beginning and/or ending points of adjoining straight and/or curve sections. Therefore, the characterization of transition section is more straightforward. The optimized heading at the ending point of the preceding straight or curve section is considered as the IH value of the transition section. Similarly, an optimal value of PAHS for a transition section is calculated using the optimized values of heading at the two end points of the transition section.

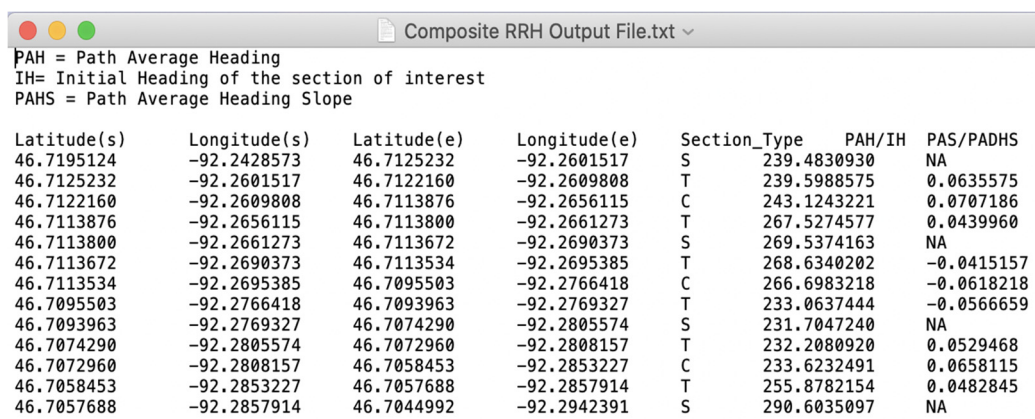


Figure 5: Screen shot of a typical output file containing optimized parameters of each section in the composite RRH.

### 3.3 Combining All Sections to Generate a Composite RRH

After identifying and characterizing each section with an optimal set of parameters, all sections are combined to generate a composite RRH for that road. The typical output file generated by the algorithm is shown in Figure 5, where each row represents an individual section of the road defined by its beginning and ending points (in terms of latitude and longitude), the optimized parameter values, and the section type. Please note that an “N” indicates that the corresponding parameter is not applicable to that section. This file has the necessary information to completely define the RRH at any point along the road and can be used to detect an unintentional lane departure in real-time using previously proposed lane departure detection method.

A composite RRH generated from a single trajectory may not be accurate for all future trajectories because usually, a vehicle will take a slightly different trajectory in each new trip on the same road. However, multiple composite RRHs obtained from different vehicle trajectories for a given road can be combined to obtain an average composite RRH. The combination of two or more composite RRHs generated from different individual GPS trajectories is achieved in two steps. First, every optimized parameter of each straight and curve section is combined using a simple average method. Second, the beginning and ending points of each straight and curve section are combined by averaging the latitude and longitude values of the beginning and ending points, separately.

After combining all straight and curve sections, transition sections are automatically combined because the beginning and ending points of all transition sections are the same as the beginning and

ending points of adjoining straight and/or curve sections as described earlier. Using the same averaging method, each additional composite RRH generated from a future vehicle trajectory can be added to an already existing average composite RRH to improve its accuracy over time.

The proposed algorithm was applied to many vehicle trajectories on the same road segment of Interstate I-35 and a composite RRH was generated from each trajectory. Three such composite RRHs generated from three different trajectories on the same road and the average composite RRH are shown in Figure 6a where heading versus distance is plotted across the entire 4.2 km length.

The difference in heading values of multiple composite RRH is not visible in Figure 6a because of the large variation of heading over the span of the road segment. To highlight the difference in different composite RRH values, a zoomed-in portion of Figure 6a marked by a red dashed circle is shown in Figure 6b. The zoomed-in portion includes the right-side portion of S2, entire T2, and the left side portion of C2 sections of the road where the difference in heading values of each composite RRH is more pronounced showing the averaging effect.

## 4 FIELD TESTS AND RESULTS

The main purpose of the proposed algorithm is to generate an average composite RRH from multiple vehicle trajectories for a given road to accurately detect unintentional lane departure in real-time using the previously developed lane departure detection method by calculating ALS at any given point on the road using equation 5, where  $h_{ref,k}$  is the RRH value at the current point,  $n$ , of the road.

$$ALS = \sum_{k=1}^n d_k \sin (h_k - h_{ref,k}) \quad (5)$$

When a vehicle unintentionally drifts away from its lane, ALS starts to increase in value (positive or negative), and once its value increases beyond a certain threshold ( $\pm 1m$ ), an unintentional lane departure is detected initiating a warning for the driver. Please note that ALS will also increase in value if a vehicle intentionally changes its lane. An intentional lane change can be distinguished from an unintentional lane departure by the presence or absence of turn signal.

In case of an intentional lane change, the increase in ALS begins to saturate upon completion of lane change because the vehicle starts to travel again in parallel to the RRH of the road. As a result of normal driving behaviour, this phenomenon i.e., the saturation of ALS can also occur in case of an unintentional wandering within a lane while ALS values remain within the  $\pm 1m$  threshold. This phenomenon is used to reset the value of ALS to zero whenever its value begins to saturate.

The accuracy of the lane departure detection method depends upon the accuracy of the composite RRH for that road. To evaluate its accuracy, field tests were performed by driving a test vehicle multiple times on the same 4.2 km segment of Interstate I-35 for which an average composite RRH was already generated using the newly proposed algorithm. The test vehicle was driven at about speed limit (70 MPH) on this 4-lane freeway and many back-and-forth lane changes were made intentionally during the field

tests. For safety reasons, intentional lane changes were made to test the accuracy of lane departure detection using the composite RRH generated by the newly proposed algorithm.

For each trip, ALS was calculated in real-time to detect any lane departure. The vehicle heading for one such test trip vs. distance is plotted along with the RRH of the road segment in Figure 7a showing that vehicle heading deviates from the RRH during each lane change as expected. The corresponding ALS vs. distance is plotted in Figure 7b showing that ALS exceeds  $\pm 1m$  threshold during each lane change. A total of ten right and left lane changes were made in this trip and all lane changes were detected accurately and in a timely manner. A digital mask for lane departure detection warning signal is plotted as a dashed red line showing the start and end of each lane change in Figure 7b. Lane departure warning signal becomes active when ALS exceeds the  $\pm 1m$  threshold and is deactivated when the vehicle heading becomes parallel to RRH of the road. In multiple field tests, more than 100 lane changes were made, and each lane change or lane departure was accurately and timely detected. Furthermore, nowhere else along the trajectory, ALS exceeded the threshold i.e., no false alarm was observed.

To test the frequency of the false alarms, the test vehicle was also driven multiple times on the same road segment without making any lane changes. In more than 10 trips on the 4.2 km long route, no false alarm was observed as indicated in Figure 7c, where ALS is plotted vs. distance for four such test trips.

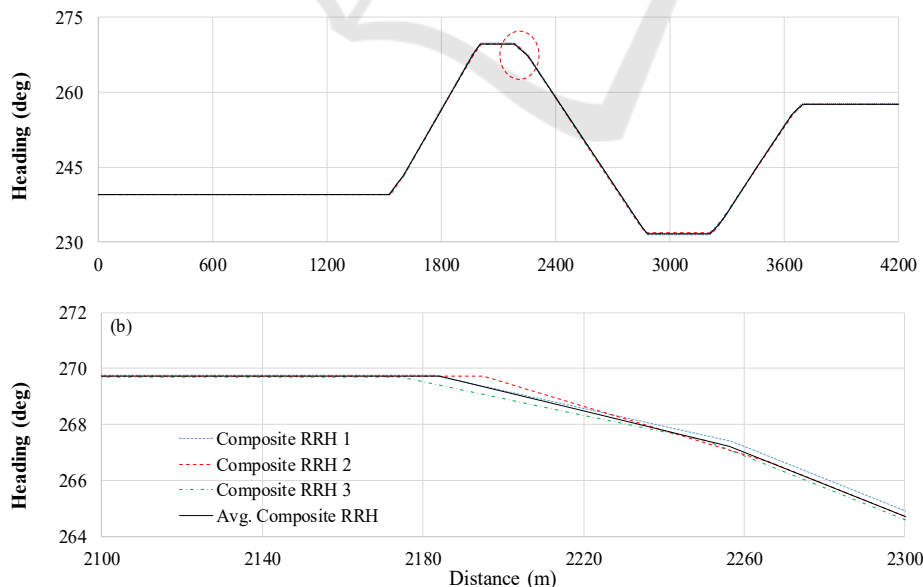


Figure 6: (a) Heading of average composite RRH and three individual composite RRH obtained from three different vehicle trajectories of 4.2 km segment of Interstate I-35, and (b) zoomed portion of (a) highlighted by red dashed circle.

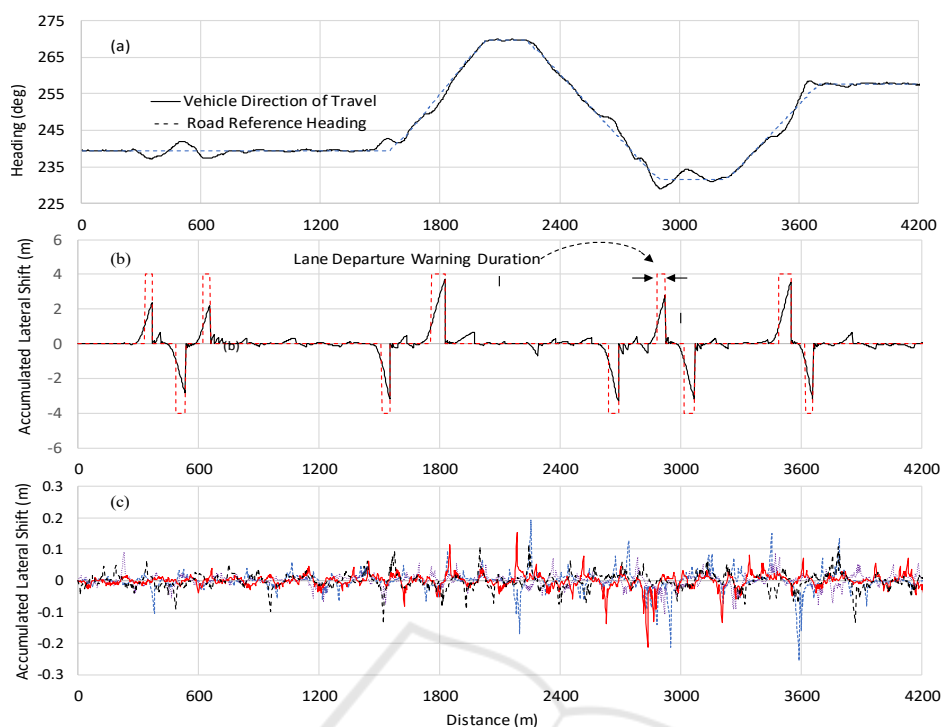


Figure 7: (a) Vehicle heading and RRH vs travelled distance for one test trial, (b) ALS versus travelled distance of the corresponding test trial trajectory, and (c) ALS versus distance on the same 4.2 km segment of Interstate I-35 for four typical trial trajectories with no lane change.

Furthermore, ALS value along any point on the road remained below  $\pm 0.3\text{m}$  which is well below the  $\pm 1\text{m}$  threshold, showing that the composite RRH generated from past vehicle trajectories significantly improves the accuracy of previously proposed lane departure detection method by practically reducing the frequency of false alarms to zero with a lot of margins to spare.

## 5 CONCLUSIONS

In this paper, a novel algorithm is proposed to generate an accurate RRH for any given road from a vehicle’s past trajectories on that road. The newly proposed algorithm can be applied to large tracts of a vehicle trajectory to generate an accurate RRH for that road regardless of whether a lane change is made during acquisition of the trajectory. The newly proposed algorithm was implemented to obtain RRH for multiple roads and integrated with the previously developed LDWS to test its ability to accurately detect unintentional lane departures. Field test results show that the newly proposed algorithm accurately detects any unintentional lane departure as well as minimizes the number of false alarms to almost zero

which was the prime objective while designing the newly proposed algorithm. Successful development of the proposed algorithm will pave the way for integration of the algorithm into one of the popular smartphone Apps.

## ACKNOWLEDGEMENTS

The authors wish to acknowledge those who made this research possible. The study was funded by the Minnesota Department of Transportation (MnDOT) and Minnesota Local Research Board (LRRB).

## REFERENCES

Driving down lane-departure crashes: A national priority, American Association of State Highway and Transportation Officials, Washington DC, 2008.  
 Cicchino, J. Effects of lane departure warning on police-reported crash rates, *Journal of Safety Research*, 2018. Volume 66, pp.61-7.  
 Salvucci, D. D. Inferring driver intent: A case study in lane-change detection. Proc. Human Factors Ergonomics Society 48th Annu. Meeting, New Orleans, LA, 2004. pp. 2228–2231.

- Kuge, N., T. Yamamura, and O. Shimoyama. A Driver Behavior Recognition Method Based on a Driver Model Framework, Warrendale, PA: Soc. Automot. Eng., 1998.
- McCall, J., and M. M. Trivedi. Visual context capture and analysis for driver attention monitoring. Proc. IEEE Conf. Intelligent Transportation Systems, Washington, DC, 2004. pp. 332–337.
- Heimes, F., and H. H. Nagel. Towards active machine-vision-based driver assistance for urban areas. *Int. J. Comput. Vision*, 2002. vol. 50, no. 1, pp. 5–34.
- Kwon, W., and S. Lee. Performance evaluation of decision-making strategies for an embedded lane departure warning system. *J. Robot. Syst.*, 2002. vol. 19, no. 10, pp. 499–509.
- An, X., M. Wu and H. He. A Novel Approach to Provide Lane Departure Warning Using Only One Forward-Looking Camera. International Symposium on Collaborative Technologies and Systems (CTS'06), 2006. pp. 356–362.
- Hsiao, P., and Chun-Wei Yeh. A Portable Real-Time Lane Departure Warning System based on Embedded Calculating Technique. IEEE 63rd Vehicular Technology Conference, Melbourne, Vic., 2006. pp. 2982–2986.
- Yu, B., W. Zhang and Y. Cai. A Lane Departure Warning System Based on Machine Vision. IEEE Pacific-Asia Workshop on Computational Intelligence and Industrial Application, Wuhan, 2008. pp. 197–201.
- Leng, Y. C., and C. L. Chen. Vision-based lane departure detection system in urban traffic scenes. 11th International Conference on Control Automation Robotics & Vision, Singapore, 2010. pp. 1875–1880.
- Lindner, P., E. Richter, G. Wanielik, K. Takagi and A. Isogai. Multi-channel lidar processing for lane detection and estimation. 12th International IEEE Conference on Intelligent Transportation Systems, St. Louis, MO, 2009. pp. 1–6.
- McCall, J. C., and M. M. Trivedi. Video-based lane estimation and tracking for driver assistance: survey, system, and evaluation. IEEE Transactions on Intelligent Transportation Systems, 2006. vol. 7, no. 1, pp. 20–37.
- Daimler Chrysler AG. Vehicle with Optical Scanning Device for a Lateral Road Area. US006038496a, 2018.
- Clanton, J. M., D. M. Bevly and A. S. Hodel. A Low-Cost Solution for an Integrated Multisensor Lane Departure Warning System. IEEE Transactions on Intelligent Transportation Systems, 2009. vol. 10, no. 1, pp. 47–59.
- Muhammad Faizan, S. Hussain and M.I. Hayee, Design And Development Of In-vehicle Lane Departure Warning System Using Standard GPS Receiver. Transportation Research Record, Journal of Transportation Research Board, I-9, 2019.
- Cao, L., and J. Krumm. From GPS traces to a routable road map. GIS: Proceedings of the 17th ACM SIGSPATIAL International Conference on Advances in Geographic Information Systems, 2009. pp. 3–12.
- Guo, T., K. Iwamura, M. Koga. Towards high accuracy road maps generation from massive GPS Traces data. IEEE International Geoscience and Remote Sensing Symposium, Barcelona, Spain, 2007.
- Chen, C., and Y. Cheng. Roads Digital Map Generation with Multi-track GPS Data. International Workshop on Education Technology and Training & International Workshop on Geoscience and Remote Sensing, Shanghai, China, 2008.
- Guo, D., S. Liu, H. Jin. A graph-based approach to vehicle trajectory analysis. *Journal of Location Based Services*, 2010. Volume 4.
- Shi, W., S. Shen, and Y. Liu. Automatic generation of road network map from massive GPS, vehicle trajectories. 12th International IEEE Conference on Intelligent Transportation Systems, St. Louis, MO, USA, 2009.
- Huang, J., M. Deng, J. Tang, S. Hu, H. Liu, S. Wariyo, and J. He. Automatic Generation of Road Maps from Low Quality GPS Trajectory Data via Structure Learning. IEEE Access (Volume – 6), 2018.